Model for Carbohydrase Action. *Aspergillus oryzae* α-Amylase Degradation of Maltotriose†

Jimmy D. Allen*,‡ and John A. Thoma

ABSTRACT: *Aspergillus oryzae* α-amylase catalyzes degradation of oligosaccharides by a variety of pathways. We present here a quantitative study of the degradation of maltotriose by this amylase. Our results lead to a scheme involving multiple transglycosylation reactions and shifted binding due to simultaneous binding of two substrate molecules. The scheme is able to account for the diverse body of information collected for the enzyme. The effect of substrate concentration on the products of maltotriose degradation is correctly predicted over a 10^4-fold concentration range, and the time course of maltotriose degradation is closely approximated by this scheme. The initial velocity data, which show deviation from Michaelis–Menton kinetics, are also consistent with the formulated scheme. The scheme is proposed as a general model of carbohydrase action.

In the previous paper (Allen & Thoma, 1978), we reported that *Aspergillus oryzae* (AO) α-amylase[1] degrades substrate maltooligosaccharides by other mechanisms in addition to unimolecular hydrolysis. The products of degradation of reducing-end labeled maltooligosaccharides depend on the initial substrate concentration and on the extent of reaction. Degradation of uniformly labeled maltotriose at high initial concentration showed that degradation is not by simple cleavage of a glycosidic bond. We concluded that, under certain experimental conditions, the mechanism of AO amylase degradation of maltooligosaccharides involves more than one substrate molecule, that is multimolecular reactions.

An examination of possible multimolecular reactions revealed that AO amylase does not catalyze condensation of two substrate molecules to any significant degree. Transglycosylations occur in the degradation of some maltooligosaccharides, but no simple transglycosylation mechanism could account for all of the experimental observations. We concluded that degradation was by some combination of transglycosylation reactions with the possibility of a two-one shifted complex (Allen & Thoma, 1978).

In this paper we report a quantitative analysis of the degradation of maltotriose by AO amylase and develop the methodology to quantitate the partitioning of intermediates by an enzyme along various possible pathways. A model emerges that is shown to account for the degradation of maltotriose by AO amylase.

Experimental Procedure

Aspergillus oryzae α-amylase was purified and reducing-end ^{14}C-labeled maltooligosaccharides were prepared as described (Allen & Thoma, 1978).

Relative Specific Acitivity Determination of Maltotriose Hydrolysate. The ^{14}C specific activity of the products of an AO amylase hydrolysis of reducing-end labeled maltotriose was determined using [^{3}H]$NaBH_4$ (McLean et al., 1973) to measure the amount of product. A series of maltotriose concentrations was prepared in 0.05 M pyridine–acetate, pH 5.3, using equal amounts of ^{14}C reducing-end labeled and varying amounts of unlabeled maltotriose. Hydrolysis was initiated by the addition of AO amylase to make 300 μL of reaction mixture. The maltotriose was allowed to achieve ca. 60% degradation of labeled maltotriose, during which time ten 10-μL aliquots were removed. The aliquots were added to 10 μL of concentrated NH_4OH and immediately spotted on Whatman 3MM paper with hot air drying. The chromatograms were developed and the ^{14}C radioactivity was counted as described (Allen & Thoma, 1978). At the end of the reaction, the remaining hydrolysate was heated at 100 °C for 10 min and stored at −15 °C.

Equal amounts of [^{3}H]$NaBH_4$ (New England Nuclear) and varying amounts of unlabeled $NaBH_4$ were prepared in 0.1 N KOH to obtain specific activities which, when used to reduce the oligosaccharides from the amylase hydrolyses, would give suitable $^{14}C/^3H$ counting ratios. Equal amounts of the diluted [^{3}H]$NaBH_4$ were added to 100 μL of amylase hydrolysate, to 100 μL of unreacted maltotriose and to 100 μL of reaction buffer. The reduction was allowed to proceed for 4 h before HCl was slowly added with cooling to obtain pH 6–7. High voltage electrophoresis (Allen & Thoma, 1978) on Whatman no. 1 or 3MM paper was used to fractionate the ^{14}C-, ^3H-labeled alditols and any unreduced aldoses. An autoradiogram was used as a guide for cutting out the electrochromatogram. Where ^{14}C compounds were absent, standards were used as a guide. The samples were eluted with water into glass scintillation counting vials, acidified with HCl to destroy any remaining [^{3}H]$NaBH_4$, and then dried in vacuo with heat. After a second acidification and drying, the final product was dissolved in 500 μL of water, and 14.5 mL of Aquasol (New England Nuclear) was added. The ^{14}C and ^3H radioactivity was determined as described (Allen & Thoma, 1978). An acid stable impurity present in [^{3}H]$NaBH_4$ (McLean et al., 1973) was corrected for by subtracting the radioactivity present in the blank. In order to normalize the specific activity, the ^{14}C to ^3H ratio in each product of degradation was divided by the

† From the Department of Chemistry, University of Arkansas, Fayetteville, Arkansas 72701. *Received June 20, 1977.* This work was supported in part by Corn Industries Research Association, by Agricultural Research Services, U.S. Department of Agriculture Grant No. 12-14-100-9908 (71), and by National Science Foundation Grant No. BMS-74-19838. A report of this work was presented at the 1976 American Society of Biological Chemists Meeting (*Fed. Proc., Fed. Am. Soc. Exp. Biol. 35,* Abstr. 2019).

‡ Current address: Department of Chemistry, University of California, Santa Barbara, Calif. 93106.

[1] Abbreviations used: AO amylase, *Aspergillus oryzae* α-amylase, 1,4-α-D-glucan glucanohydrolase, EC 3.2.1.1; G_n, a maltodextrin of *n* glucosyl units; G_n*, a reducing-end ^{14}C-labeled maltodextrin of *n* glucosyl units; ′, an enzyme–substrate intermediate.

0006-2960/78/0417-2345$01.00/0

TABLE I: Reducing-End Labeled Maltotriose Degradation Products as a Function of Concentration.

Initial $[G_3^*]$ (mM)	Extent of reaction[a]	$[G_1^*]/[G_2^*]$	AO amylase hydrolysate normalized spec act.[b] Maltotriose	Maltose	Glucose	Partitioning of intermediates[c] f_a	f_b
0.5	0.57	*c*	0.99	0.09[d]	1.01	~1.00	~1.00
1.6	0.57	5.1	0.90	0.15[d]	0.99	0.91	1.00
5.0	0.59	2.7	0.84	0.31	1.01	0.94	0.78
16.0	0.61	1.1	0.82	0.52	1.02	0.80	0.67
50.0	0.67	0.58	0.82	0.66	0.94	0.67	0.50

[a] $([G_1^*] + [G_2^*])/([G_1^*] + [G_2^*] + [G_3^*])$. [b] The reduction in ^{14}C specific activity due to the production of unlabeled products, calculated as (product: ^{14}C dpm/^3H dpm)/(substrate: ^{14}C dpm/^3H dpm) after $[^3H]NaBH_4$ reduction. [c] Little G_2^* is formed so that this ratio has too much error to be significant. [d] Because the production of G_2 was much greater than G_2^*, the ^3H counts were much larger than the ^{14}C counts. Consequently, these determinations have more experimental uncertainty than the corresponding values at higher substrate concentrations. [e] Refer to Figure 1.

TABLE II: Predicted Product Specific Activity Resulting from Degradation of Maltotriose through Various Pathways.

Mechanism[a]	Extent of reaction	Rel spec act.[b] Maltotriose	Maltose	Glucose
Unimolecular hydrolysis	*c*	1	0	1
Two-one shifted binding with hydrolysis	*c*	1	1	0
Glucosyl transfer	*c*	1	0.67	*d*
Maltosyl transfer[e]	0.25	0.95	0.23	0.97
	0.50	0.87	0.23	0.94
	0.75	0.76	0.22	0.90

[a] The mechanisms are diagrammed in Figure 4 of the preceding paper (Allen & Thoma, 1978). [b] Product specific activity divided by original substrate specific activity. [c] The specific activities are independent of the extent of reaction. [d] No glucose is formed. [e] The method of calculation can be found in the supplementary material (see paragraph concerning supplementary material at the end of this paper).

^{14}C to ^3H ratio in the original substrate maltotriose for each reaction.

Initial Velocity Measurements. A series of reducing-end labeled maltotriose concentrations was prepared in 0.05 M pyridine-acetate, pH 5.3, buffer. Reaction was initiated by addition of AO amylase, and the mixture was incubated at 25 °C. Aliquots, ten for each concentration, were removed as a function of time and added to an equal volume of concentrated NH_4OH before spotting on 3MM paper with hot air drying. The chromatograms were developed and visualized, and the radioactivity was counted (Allen & Thoma, 1978). From the fraction of labeled maltotriose degraded and the initial substrate concentration, the concentration of total product was calculated for each aliquot. The concentration of products was plotted against time and the initial velocity determined by extrapolation.

Results

Analyses of Maltotriose Hydrolysates. The ratios of labeled products and the relative specific activities of the sugars produced in degradation of reducing-end labeled maltotriose are given in Table I as a function of substrate concentration. The specific activities have been normalized to the starting substrate maltotriose so that a specific activity of less than unity is due to the production of unlabeled sugar. At low substrate concentrations, where unimolecular hydrolysis dominates, reducing-end labeled maltotriose is cleaved almost exclusively at the reducing-end glycosidic bond to yield unlabeled maltose and labeled glucose. As the starting maltotriose concentration is raised, production of maltose from the reducing end of the maltotriose by the multimolecular mechanism is shown by an increase in maltose specific activity and a decrease in the ratio of labeled glucose to labeled maltose. The specific activity of glucose is relatively insensitive to substrate concentration indicating that neither the unimolecular or multimolecular pathways produce much unlabeled glucose. In addition, Table I shows that, at the higher initial substrate concentrations, the substrate maltotriose specific activity is decreased during the course of the reaction, indicating that unlabeled maltotriose is produced by the multimolecular reaction.

Minimal Model. Table II shows how the specific activities of the oligosaccharides depend on the degradation mechanism. Note that only maltosyl transfer can account for a depression in the specific activity of maltotriose. Hence, we know that a minimal model for trisaccharide degradation must include a maltosyl transfer pathway. However, we showed earlier (Allen & Thoma, 1978) that maltosyl transfer alone cannot account for the large amount of labeled maltose seen at the highest substrate concentrations. Either shifted binding or glucosyl transfer would be necessary to account for the high degree of labeled maltose production. Table II shows that two-one shifted binding followed by unimolecular hydrolysis predicts a reduction of glucose specific activity. The slight reduction in glucose specific activity seen at the highest substrate concentration (Table I) is attributable to maltosyl transfer (Table II). Thus, for a minimal mechanism the enzyme acts as a hydrolase and a transferase, transferring either glucosyl or maltosyl residues.

The unimolecular hydrolysis pathways and the transfer pathways are linked through a common substrate and common intermediates. Assuming that these common intermediates form a single pool leads directly to the degradation scheme shown in Figure 1. Thus, unimolecular hydrolysis and transfer pathways form an interlocking network and must be considered as integrated rather than independent pathways. Note that unimolecular hydrolysis occurs along pathway 1·9·11 (see Figure 1 legend for nomenclature), maltosyl transfer by pathway 1·9·13·15·17, and glucosyl transfer by pathway 1·3·5·7·11. Figure 1 also reveals a double transfer pathway, 1·3·5·7·13·15·17, with glucosyl transfer followed by maltosyl transfer.

For simplicity, the scheme in Figure 1 describes initial steady-state kinetics so that steps in which products are formed are considered only in the forward direction. The EG_1' complex is shown to only undergo transfer and not hydrolysis as we will explain below. In step 5, G_3^* binds reversibly to the EG_1' complex to give $EG_1'{\cdot}G_3^*$ which can then react to give EG_4^*.

Once the new glycosidic bond is formed, however, the reaction is not reversible since EG_4* only fragments to yield EG_2' and G_2* in step 7 (Allen & Thoma, 1978). In step 13, G_3* will bind reversibly to EG_2' to give EG_2'·G_3* which can react to give EG_5*. In this case, however, the glycosidic bond will cleave to give EG_2'·G_3* since a normal breakdown of G_5* gives G_2 and G_3* (pathway 14·11). The EG_4* and EG_5* complexes can also dissociate to E + G_4* and E + G_5*, respectively, but G_4* and G_5* are consumed so rapidly that they are never seen experimentally.

We can use the information in Table I to quantify the maltotriose degradation for the substrate concentrations examined. A mathematical analysis is detailed in the supplementary material (see paragraph concerning supplementary material at the end of this paper); we will briefly outline the method here. Partitioning of intermediates EG_3* and EG_2' regulates what fraction of substrate flows along the various pathways. Turning first to EG_3*, we define the fraction of EG_3* that partitions forward along step 9 as f_a and that which partitions by pathway 3·5·7 as $1 - f_a$. Pathways 3·5·7 and 9 can be simplified to

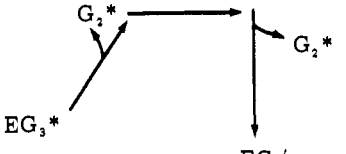

(1)

and

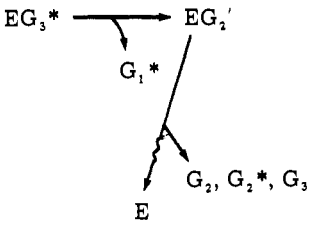

(2)

respectively. For calculation of f_a, the fate of EG_2' is irrelevant and we have simply considered the sum of the EG_2' degradation pathways. The distinction between these schemes is that, whereas pathway 3·5·7 (eq 1) produces only G_2 and G_2*, pathway 9 (eq 2) also produces G_1*. Hence the ratio of G_1* to G_2 + G_2* was used to calculate the values of f_a given in Table I.

We turn now to degradation of EG_2' and a determination of the partitioning between pathway 11 (f_b) and pathway 13·15·17 ($1 - f_b$). Pathways 11 and 13·15·17 may be represented as

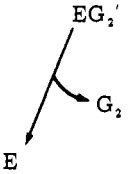

(3)

and

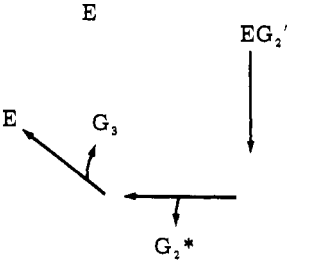

(4)

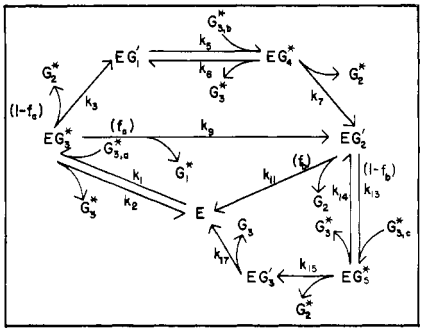

FIGURE 1: Maltotriose degradation scheme. E, AO α-amylase; k, rate constant, a prime indicates an enzyme–glycosyl complex. The G_3* subscripts indicate the point at which they enter the degradation scheme. The steps and pathways in this scheme are referred to by rate constant index numbers. The fraction of EG_3* degraded to EG_2' via pathway 9 and via pathway 3·5·7 is f_a and $1 - f_a$, respectively. Similarly, the fraction of EG_2' degraded to E by pathway 11 and via pathway 13·15·17 is f_b and $1 - f_b$, respectively. Additional steps required to account for all of the experimental data are shown in Figure 2.

respectively. The distinguishing characteristic between the two pathways is that pathway 11 produces G_2, whereas pathway 13·15·17 produces only G_2*. Consequently, the specific activity of maltose was used to calculate the values of f_b given in Table I.

Since we have calculated the partitioning of intermediates EG_3* and EG_2' for the maltotriose concentrations examined in Table I, we can calculate the fraction of substrate maltotriose that is consumed in the various steps in the degradation model. We have conceptually divided the substrate maltotriose into three pools designated by subscripts a, b, and c as shown in Figure 1. At the lower concentration the only degradation is unimolecular hydrolysis, pathway 1·9·11, so that $f_a = f_b = 1$ and all of the maltotriose enters the scheme in step 9 (G_3*$_a$). As the maltotriose concentration is increased, the fraction of maltotriose degraded by the multimolecular pathways increases. Consequently, $1 - f_a$ and $1 - f_b$ are increased so that maltotriose begins to enter the scheme in the bimolecular steps, 5 (G_3*$_b$) and 13 (G_3*$_c$).

The scheme has some apparent discrepancies that are related and can be resolved by inclusion of an addition mechanism. First, as we pointed out above, the EG_1' produced in step 3 only undergoes transfer and not hydrolysis, whereas EG_2' produced in step 9 can either undergo hydrolysis or transfer. Second, the model predicts that G_2* will be produced at low substrate concentrations since step 3 is independent of maltotriose concentration. However, we find experimentally that at low substrate concentrations the production of G_2* is negligible. Third, the formation of the positional isomer that leads to the production of the EG_1' complex is energetically unfavorable because of the subsite energies (Allen & Thoma, 1976, 1978) so that EG_1' should not normally form. Finally, the model predicts that partitioning between pathway 3·5·7 and pathway 9 is independent of maltotriose concentration. The partitioning along pathway 3·5·7 can be expressed as

$$1 - f_a = \frac{v_3}{v_3 + v_9} = \frac{k_9}{k_3 + k_9} \qquad (5)$$

where v_3 is the velocity of degradation of EG_3* along pathway 3·5·7 (k_3[EG_3*]) and v_9 is the velocity of degradation of pathway 9 (k_9[EG_3*]). Equation 5 predicts that $1 - f_a$ will be independent of the concentration of maltotriose, while the results in Table I clearly show that this function depends on maltotriose concentration.

These discrepancies are all resolved if a second substrate

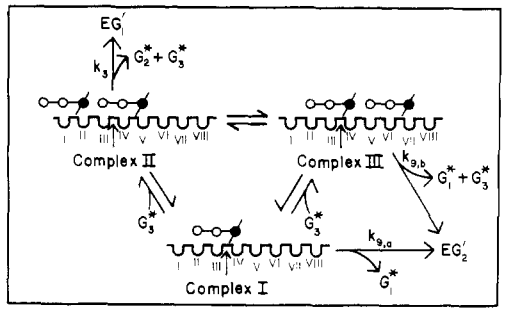

FIGURE 2: Two-one binding in the degradation of maltotriose. O—O—●, reducing-end ^{14}C labeled maltotriose; ∪, subsite on the enzyme corresponding to a glucopyranoside unit binding position; ↑, bond cleavages site. This mechanism is an integral part of the model in Figure 1. The EG_3^* complex in Figure 1 is actually a composite of complexes I, II, and III. EG_1', EG_2', and k_3 are identical with their corresponding symbols in Figure 1. The rate constant k_9 in Figure 1 is now proportioned between $k_{9,a}$ and $k_{9,b}$. The enzyme is composed of eight subsites as shown (Allen & Thoma, 1976). Maltotriose molecules that are bound so as to expose a susceptible bond to the catalytic amino acids are referred to as productively bound.

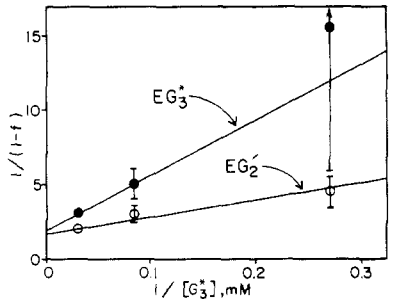

FIGURE 3: Double-reciprocal plots for the partitioning of intermediates between two branch points in the maltotriose degradation scheme (Figure 1). (●) partitioning of EG_3^*; (O) partitioning of EG_2'. The vertical bars are an estimate of error. The lines are least-squares fits weighted by the reciprocal of the variance. The maltotriose concentrations have been adjusted to take into account the high extent of reaction (Lee & Wilson, 1971; supplementary material (see paragraph at the end of this paper concerning supplementary material)). The values of f_a and f_b measured at the lower substrate concentrations are not used because of excessive experimental scatter (footnote *d* in Table I).

maltotriose can bind to EG_3^* leading to two-one shifted binding *with transfer* as shown in Figure 2. At low substrate concentrations, complex I predominates and almost all of the substrate flows along pathway 9a. As the concentration of substrate maltotriose is raised, the probability of two maltotriose molecules being bound simultaneously increases and complexes II and III become populated. The binding of two maltotriose molecules in complex III does not perturb the productively bound substrate so that fragmentation still leads to EG_2' by step 9b. However, the binding of two maltotriose molecules in complex II causes a shift in the productively bound maltotriose so that the nonreducing glycosidic bond is exposed to the catalytic amino acids. Fragmentation of complex II leads to EG_1' through step 3. At saturating substrate concentrations the proportioning of the EG_3^* complex in Figure 2 between pathway 9 and pathway 3·5·7 is determined by the concentration of complexes II and III and their respective rate constants.

This two-one shifted binding accounts for all of the discrepancies in the model. First, EG_1' chiefly undergoes transfer because complex II is formed only at high substrate concentrations where transglycosylation is favored. Second, G_2^* is not produced at low substrate concentrations since the nonreducing-end bond is exposed to cleavage only at high substrate concentrations. Third, we can now see how at high substrate concentrations the energetics of binding can be such that formation of EG_1' can be favorable. At low substrate concentrations, the population of the positional isomers leading to an EG_2' complex or an EG_1' complex is determined by the binding energies of subsites II–IV vs. subsites III–V. Since subsite II has a much more favorable binding energy than subsite V, the EG_2' complex dominates (Allen & Thoma, 1976). However, at high substrate concentrations the population of complexes II and III will be determined by the binding energies for subsites I–V and II–VII, respectively. The binding energies of these two sets of subsites are such that neither complex is strongly favored over the other (Allen & Thoma, 1976) so that formation of EG_1' is allowed. Lastly, the involvement of two maltotriose molecules in the shifted mechanism accounts for the dependence of $1 - f_a$ on substrate concentration. In fact, the model now predicts that the double-reciprocal plot of $1/(1 - f_a)$ vs. $1/[G_3^*]$ as shown in Figure 3 will be rectilinear. With the available data, it is impossible to conclude that the plot is rectilinear. However, as we will show below, data obtained from the plot account for the experimental observations.

Turning now to partitioning of EG_2' degradation, we find that f_b is also a function of maltotriose concentration (Table I) as predicted by the model (Figure 1). By a steady analysis (Cleland, 1975), the fraction of EG_2' degraded through pathway 13·15·17 reduces to the double-reciprocal form

$$\frac{1}{1 - f_b} = \frac{k_{11}(k_{14} + k_{15})}{k_{13}k_{15}[G_3^*]} + 1 \qquad (6)$$

Equation 6 predicts that the plot shown in Figure 3 should be rectilinear with a vertical intercept of unity, which implies that at saturating maltotriose concentration all EG_2' will be diverted through pathway 13·15·17. Yet, a least-squares line has an intercept of 1.7, statistically different from unity. Hence, not all of the EG_2' is diverted through pathway 13·15·17 at saturating substrate concentrations, which can be accounted for by introducing an equilibrium step in pathway 13·15·17 before the entry of maltotriose, $G_3^*{}_c$. Such an equilibrium would occur if the EG_2' complex must isomerize to EG_2'' before reaction with the G_3^* to form EG_5^*. We will show below that the plots of Figure 3 do have predictive value.

Prediction of Experimental Data. Knowing how f_a and f_b depend on the substrate concentration (Figure 3), we can quantitatively partition maltotriose along the multiple pathways in Figure 1 and compute the products of hydrolysis at any given substrate concentration. The detailed procedure for these calculations is set forth in the supplementary material. The test of our model will lie in its ability to correctly predict the experimental data. The experimentally determined product ratios from reducing-end labeled maltotriose degradation are plotted in Figure 4 and the theoretical lines are computed from the model. Even though f_a and f_b were determined at maltotriose concentrations of 5–50 mM (Table I), the model correctly predicts the experimental product ratios within 0.05 at 500 mM maltotriose concentration, approaching substrate saturation. An additional test of the model is provided by the time course of maltotriose degradation (Figure 1 in Allen & Thoma, 1978). The model-predicted shift in the product ratios due to the shift from multimolecular to unimolecular mechanisms as the substrate is depleted closely approximates the experimental data (not shown).

Initial Velocity Kinetics. When the initial velocities for AO amylase degradation of maltotriose are plotted as a function of substrate concentration, a sigmoidal curve is obtained (not shown). A double-reciprocal plot in Figure 5 shows that the

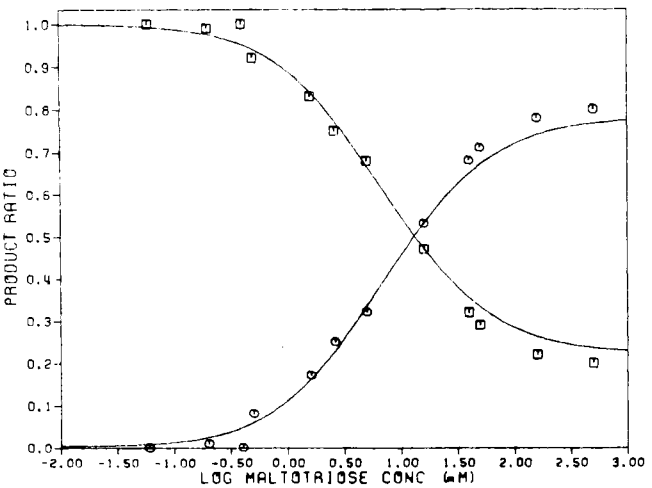

FIGURE 4: Effect of maltotriose concentration on the product ratio. The experimental initial product ratios from reducing-end labeled maltotriose degradation are shown as a function of initial maltotriose concentration (mM) (Allen & Thoma, 1978) for (□) $[G_1^*]/([G_1^*] + [G_2^*])$ and (○) $[G_2^*]/([G_1^*] + [G_2^*])$. The line is calculated from the model.

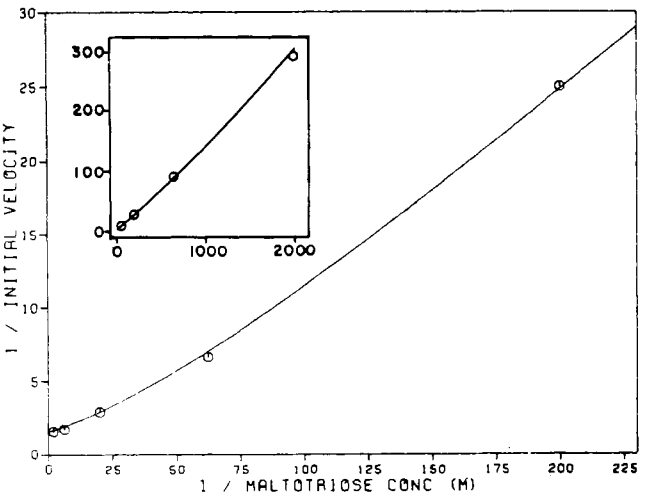

FIGURE 5: Double-reciprocal plot for the initial velocity of maltotriose degradation. The inset is a compression of the axes in order to show the points determined at low substrate concentrations. The line is a least squares fit (Cleland, 1967), weighted by the reciprocal of the square of the velocities, to eq 7. The calculated constants in eq 7 are: α_1, 6.4; α_2, 822; β_1, 53; β_2, 1210.

enzyme does not follow Michaelis-Menton kinetics. An asymptote is approached at low substrate concentrations that intersects the vertical axis at a negative value implying that the velocity equation is at least second order with respect to substrate in both numerator and denominator or a 2:2 function[2] (Bardsley & Childs, 1975).

The method of King & Altman (1956) was applied to the scheme for maltotriose degradation shown in Figure 1. The initial steady-state velocity equation is

$$v_0 = -\frac{d[G_3^*]}{dt} = \frac{\alpha_1[G_3^*] + \alpha_2[G_3^*]^2}{1 + \beta_1[G_3^*] + \beta_2[G_3^*]^2} \qquad (7)$$

where α_1, α_2, β_1, and β_2 are complex constants.

Equation 7, having the required 2:2 form, was fitted to the initial velocity data using a weighted least-squares analysis (Cleland, 1967), and the resulting equation is plotted in Figure 5. The good fit to the experimental data provides confirming evidence that our model adequately accounts for the mechanism of maltotriose degradation. However, we cannot exclude a function more complex than 2:2 since it might also account for the initial velocity data (Bardsley & Childs, 1975).

Discussion

We assumed in this development that the enzyme reacts through an enzyme-glycosyl intermediate formed from the nonreducing end of the substrate molecule. Although AO amylase has not specifically been shown to react through such an intermediate, enzyme-glycosyl intermediates are well documented for other carbohydrases (Legler, 1968; Chipman et al., 1968; Dahlquist et al., 1969; Voet & Abeles, 1970; Huber & Thompson, 1973). However, some workers have proposed that glycosylases react through formation of a ternary complex (Jermyn, 1962a,b; Nakamura, 1970; Umezurike, 1975) where donor and acceptor are present on the enzyme surface at the same time. This proposal was based on kinetic studies and on the observation that transfer of an identical group is influenced by the structure of the donor molecule. It has been shown that the sulfur transferring enzyme rhodanese, which reacts through an obligatory enzyme-sulfur intermediate, exhibits different reactivity as a function of the donor substrate (Jarabak & Westley, 1974). It was proposed that the enzyme has a "memory" of its donor substrate, possibly as a consequence of a conformational change. A similar enzymic "memory" phenomenon has been proposed for α-amylase (Thoma et al., 1971). Enzymic "memory" could possibly account for the effects that led to the proposal of a glycosylase ternary complex. The necessary introduction of an isomerization of EG_2' to EG_2'' to account for the saturation kinetics of the AO amylase model might well be a consequence of a conformational "memory".

Although there have been several reports of multimolecular reactions catalyzed by carbohydrases, the studies are generally qualitative. Only a few attempts have been made to quantitate these multimolecular reactions. Chipman (1971) proposed a kinetic model for lysozyme transglycosylation reactions and showed that the model adequately fit the experimental data. Robyt & French (1970) carried out a quantitative study of the multimolecular reactions catalyzed by porcine pancreatic α-amylase and developed a "square plot" to estimate the product ratios for unimolecular and multimolecular conditions. As detailed elsewhere (Allen, 1975), the "square plot" did not prove satisfactory to describe AO amylase, and the results reached for porcine pancreatic α-amylase may need to be reexamined. The amylase model developed here accounts for the product ratios, time course, and initial velocity data for maltotriose degradation. The experimental protocol used here for the study of AO amylase action should be applicable to other carbohydrases showing multiple catalytic activities. With modifications to take into account reactions such as condensation, the model should have general applicability in explaining the action of carbohydrases.

Supplementary Material Available

The analysis of maltosyl transfer used to calculate the specific activities of Table II and a detailed analysis of the calculation of f_a and f_b of Figure 1 (15 pages). Ordering information is given on any current masthead page.

References

Allen, J. D. (1975) Ph.D. Thesis, University of Arkansas.
Allen, J. D., & Thoma, J. A. (1976) *Biochem. J. 159,* 121.

[2] Cleland (1970) refers to this type of velocity equation as a 2/1 function because in its double-reciprocal form the numerator is a second order and the denominator is first order in substrate.

Allen, J. D., & Thoma, J. A. (1978) *Biochemistry 17* (preceding paper in this issue).
Bardsley, W. G., & Childs, R. E. (1975) *Biochem. J. 149,* 313.
Chipman, D. M. (1971) *Biochemistry 10,* 1714.
Chipman, D. M., Pollock, J. J., & Sharon, N. (1968) *J. Biol. Chem. 243,* 487.
Cleland, W. W. (1967) *Adv. Enzymol. 29,* 1-32.
Cleland, W. W. (1970) *Enzymes, 3rd Ed. 2,* 1-65.
Cleland, W. W. (1975) *Biochemistry 14,* 3220.
Dahlquist, F. W., Rand-Meir, T., & Raftery, M. A. (1969) *Biochemistry 8,* 4214.
Huber, R. E., & Thompson, D. J. (1973) *Biochemistry 12,* 4011.
Jarabak, R., & Westley, J. (1974) *Biochemistry 13,* 3237.
Jermyn, M. A. (1962a) *Aust. J. Biol. Sci. 15,* 233.
Jermyn, M. A. (1962b) *Aust. J. Biol. Sci. 15,* 248.
King, E. L., & Altman, C. (1956) *J. Phys. Chem. 60,* 1375.
Lee, H., & Wilson, I. B. (1971) *Biochim. Biophys. Acta 242,* 519.
Legler, G. (1968) *Biochim. Biophys. Acta 151,* 728.
McLean, C., Werner, D. A., & Aminoff, D. (1973) *Anal. Biochem. 55,* 72.
Nakamura, L. K. (1970) *Can. J. Biochem. 48,* 1260.
Robyt, J. F., & French, D. (1970) *J. Biol. Chem. 245,* 3917.
Thoma, J. A., Spradlin, J. E., & Dygert, S. (1971) *Enzymes, 3rd Ed. 5,* 115-189.
Umezurike, G. M. (1975) *Biochim. Biophys. Acta 397,* 164.
Voet, J. G., & Abeles, R. H. (1970) *J. Biol. Chem. 245,* 1020.

Enzymatic Preparation of the 5′-Triphosphates of 2′-Deoxytubercidin, 2′-Deoxytoyocamycin, and 2′-Deoxyformycin and the Allosteric Effects of These Nucleotides on Ribonucleotide Reductase†

Shirley A. Brinkley, Arthur Lewis, Walter J. Critz, Linda L. Witt, Leroy B. Townsend, and Raymond L. Blakley*

ABSTRACT: Analogues of 2′-deoxyadenosine are potentially of interest as chemotherapeutic agents since the corresponding 5′-triphosphates are expected to mimic the action of dATP in causing allosteric inhibition of mammalian ribonucleotide reductase, but to be metabolically more stable than dATP. A synthetic route to analogues of dATP via preparative reduction of some ATP analogues is described, which could be used for large scale preparation of the dATP analogues and the corresponding 2′-deoxyribonucleosides. The naturally occurring nucleosides tubercidin, toyocamycin, and formycin have been converted to the corresponding 5′-triphosphates by published procedures and purified by ion-exchange chromatography. Tubercidin triphosphate has been reduced to 2′-deoxytubercidin 5′-triphosphate (dTuTP) enzymatically in the presence of the ribonucleotide reductase from *Lactobacillus leichmannii* with about 90% yield. After purification by chromatography on an organoborate column and by ion-exchange chromatography on DEAE-cellulose the recovery of dTuTP was about 76% with 9% recovery of unreacted tubercidin triphosphate. In the absence of allosteric activators, toyocamycin triphosphate (ToTP) and formycin triphosphate (FTP) are not reduced by the *L. leichmannii* reductase, although FTP binds to the catalytic site as shown by its linear competitive inhibition of the reduction of ATP, GTP, and UTP with inhibition constants in the range 0.3 to 0.6 mM. However, in the presence of 1 mM dGTP, FTP is reduced at about the same rate as ATP, and ToTP at about half this rate. With FTP as substrate the true K_m for dGTP is 0.029 ± 0.011 mM and the kinetically determined dissociation constant 0.106 ± 0.033 mM. In the presence of 0.5 mM dGTP the yield of dFTP from the organoborate column averaged 49% with recovery of 39% of the original FTP. dGTP was largely separated from dFTP on this column. dTuTP, dFTP, and dToTP are all able to mimic dATP as activators of CTP reduction by the *L. leichmannii* reductase. The kinetically determined dissociation constants for the enzyme-activator complexes and for the enzyme-CTP-activator complexes indicate that dTuTP, dToTP, and dFTP all bind to the allosteric site with about the same affinity as dATP.

A number of considerations suggest that ribonucleotide reductase is the rate-limiting enzyme in DNA biosynthesis. The enzyme is present at very low levels in vertebrate tissues, but activity rapidly increases when the tissue commences proliferation. Thus Larsson (1969) and King & Lancker (1969) have shown that a short period after partial hepatectomy of rats there is a rapid increase in reductase activity in the regenerating liver that progresses for 20-30 h. Other rapidly proliferating cells such as Yaba poxvirus tumor (Gordon & Fiel, 1969), leukemic mouse spleen (Fujioka & Silber, 1970), and Ehrlich ascites tumor (Cory & Whitford, 1972) show a similar correlation between cell growth and ribonucleotide reductase activity. There is also a strict parallelism between the measured levels of ribonucleotide reductase and the fraction of L-cells that are synthesizing DNA (Turner et al., 1968). An even more impressive report is that of Elford et al. (1970) who studied the level of ribonucleotide reductase activity in a series of minimum deviation hepatomas. They

† From the Department of Biochemistry, College of Medicine, University of Iowa, Iowa City, Iowa 52242, and the Department of Biopharmaceutical Sciences, College of Pharmacy, University of Utah, Salt Lake City, Utah 84112. *Received December 22, 1977.* This research was supported by United States Public Health Service Research Grant CA 16254 and Research Contracts N01-CM-43806 and CM-77142 from the Division of Cancer Treatment NCI, National Institutes of Health, Department of Health Education and Welfare.

0006-2960/78/0417-2350$01.00/0